

University of Groningen

## A European-wide (222)radon and (222)radon progeny comparison study

Schmithuesen, Dominik; Chambers, Scott; Fischer, Bernd; Gilge, Stefan; Hatakka, Juha; Kazan, Victor; Neubert, Rolf; Paatero, Jussi; Ramonet, Michel; Schlosser, Clemens

*Published in:*  
Atmospheric Measurement Techniques

*DOI:*  
[10.5194/amt-10-1299-2017](https://doi.org/10.5194/amt-10-1299-2017)

**IMPORTANT NOTE:** You are advised to consult the publisher's version (publisher's PDF) if you wish to cite from it. Please check the document version below.

*Document Version*  
Publisher's PDF, also known as Version of record

*Publication date:*  
2017

[Link to publication in University of Groningen/UMCG research database](#)

### *Citation for published version (APA):*

Schmithuesen, D., Chambers, S., Fischer, B., Gilge, S., Hatakka, J., Kazan, V., Neubert, R., Paatero, J., Ramonet, M., Schlosser, C., Schmid, S., Vermeulen, A., & Levin, I. (2017). A European-wide (222)radon and (222)radon progeny comparison study. *Atmospheric Measurement Techniques*, 10(4), 1299-1312. <https://doi.org/10.5194/amt-10-1299-2017>

### **Copyright**

Other than for strictly personal use, it is not permitted to download or to forward/distribute the text or part of it without the consent of the author(s) and/or copyright holder(s), unless the work is under an open content license (like Creative Commons).

The publication may also be distributed here under the terms of Article 25fa of the Dutch Copyright Act, indicated by the "Taverne" license. More information can be found on the University of Groningen website: <https://www.rug.nl/library/open-access/self-archiving-pure/taverne-amendment>.

### **Take-down policy**

If you believe that this document breaches copyright please contact us providing details, and we will remove access to the work immediately and investigate your claim.

*Downloaded from the University of Groningen/UMCG research database (Pure): <http://www.rug.nl/research/portal>. For technical reasons the number of authors shown on this cover page is limited to 10 maximum.*



# A European-wide $^{222}\text{Rn}$ and $^{222}\text{Rn}$ progeny comparison study

Dominik Schmuthüsen<sup>1</sup>, Scott Chambers<sup>2</sup>, Bernd Fischer<sup>3</sup>, Stefan Gilge<sup>4</sup>, Juha Hatakka<sup>5</sup>, Victor Kazan<sup>6</sup>, Rolf Neubert<sup>7</sup>, Jussi Paatero<sup>5</sup>, Michel Ramonet<sup>6</sup>, Clemens Schlosser<sup>8</sup>, Sabine Schmid<sup>8</sup>, Alex Vermeulen<sup>9,a</sup>, and Ingeborg Levin<sup>1</sup>

<sup>1</sup>Institut für Umweltphysik (IUP), Heidelberg University, Heidelberg, Germany

<sup>2</sup>Institute for Environmental Research (ANSTO), Lucas Heights, Australia

<sup>3</sup>Umweltbundesamt (UBA), Meßstelle Schauinsland, Oberried, Germany

<sup>4</sup>Deutscher Wetterdienst, Hohenpeißenberg (HPB), Hohenpeißenberg Germany

<sup>5</sup>Finnish Meteorological Institution (FMI), Helsinki, Finland

<sup>6</sup>Laboratoire des Sciences du Climat et de l'Environnement, LSCE/IPSL, CEA-CNRS-UVSQ, Université Paris-Saclay, Gif-sur-Yvette, France

<sup>7</sup>Centrum voor IsotopenOnderzoek (CIO), ESRIG, University of Groningen, Groningen, the Netherlands

<sup>8</sup>Bundesamt für Strahlenschutz (BfS), Freiburg, Germany

<sup>9</sup>Energy research Centre of the Netherlands (ECN), Petten, the Netherlands

<sup>a</sup>now at: ICOS ERIC – Carbon Portal, Lund, Sweden

Correspondence to: Ingeborg Levin (ingeborg.levin@iup.uni-heidelberg.de)

Received: 1 April 2016 – Discussion started: 24 August 2016

Revised: 28 February 2017 – Accepted: 12 March 2017 – Published: 3 April 2017

**Abstract.** Although atmospheric  $^{222}\text{Rn}$  ( $^{222}\text{Rn}$ ) activity concentration measurements are currently performed worldwide, they are being made by many different laboratories and with fundamentally different measurement principles, so compatibility issues can limit their utility for regional-to-global applications. Consequently, we conducted a European-wide  $^{222}\text{Rn}/^{222}\text{Rn}$  progeny comparison study in order to evaluate the different measurement systems in use, determine potential systematic biases between them, and estimate correction factors that could be applied to harmonize data for their use as a tracer in atmospheric applications. Two compact portable Heidelberg radon monitors (HRM) were moved around to run for at least 1 month at each of the nine European measurement stations included in this comparison. Linear regressions between parallel data sets were calculated, yielding correction factors relative to the HRM ranging from 0.68 to 1.45. A calibration bias between ANSTO (Australian Nuclear Science and Technology Organisation) two-filter radon monitors and the HRM of  $\text{ANSTO}/\text{HRM} = 1.11 \pm 0.05$  was found. Moreover, for the continental stations using one-filter systems that derive atmospheric  $^{222}\text{Rn}$  activity concentrations from measured atmospheric progeny activity concentrations, prelim-

inary  $^{214}\text{Po}/^{222}\text{Rn}$  disequilibrium values were also estimated. Mean station-specific disequilibrium values between 0.8 at mountain sites (e.g. Schauinsland) and 0.9 at non-mountain sites for sampling heights around 20 to 30 m above ground level were determined. The respective corrections for calibration biases and disequilibrium derived in this study need to be applied to obtain a compatible European atmospheric  $^{222}\text{Rn}$  data set for use in quantitative applications, such as regional model intercomparison and validation or trace gas flux estimates with the radon tracer method.

## 1 Introduction

$^{222}\text{Rn}$  ( $^{222}\text{Rn}$ ) is a short-lived radioactive noble gas (half-life time  $T_{1/2} = 3.8$  days), which is produced in all soils from the radioactive decay of  $^{226}\text{Ra}$  (a member of the primordial  $^{238}\text{U}$  decay series).  $^{222}\text{Rn}$  is the first gaseous constituent in this series and therefore has a chance of escaping from the (unsaturated) soil zone into the atmosphere by diffusion. The exhalation rate of  $^{222}\text{Rn}$  from continental surfaces depends on the soil properties, mainly  $^{226}\text{Ra}$  content, grain size distribution, porosity, and moisture content

(e.g. Nazaroff, 1992; Karstens et al., 2015). The  $^{222}\text{Rn}$  flux from (ocean) water surfaces is negligible (Schery and Huang, 2004) compared to that from continental soils; therefore, the atmospheric  $^{222}\text{Rn}$  activity concentration can serve as a (qualitative) tracer to distinguish continental from marine air masses (e.g. Dörr et al., 1983; Polian et al., 1996). If the continental  $^{222}\text{Rn}$  exhalation rate and its spatial and temporal distribution are known,  $^{222}\text{Rn}$  can also serve as a quantitative tracer for atmospheric boundary layer mixing and transport model validation (e.g. Jacob and Prather, 1990; Jacob et al., 1997; Taguchi et al., 2011; Williams et al., 2011).

Due to its increasing use as a quantitative tracer in atmospheric modelling or to estimate greenhouse gas fluxes with the radon tracer method (e.g. Levin et al., 1999), the number of atmospheric  $^{222}\text{Rn}$  measurements has greatly increased worldwide. Two fundamentally different analysis systems have been in operation across the European radon monitoring network in the last decade: (i) dual-flow-loop two-filter monitors (Whittlestone and Zahorowski, 1998; Chambers et al., 2011), which sample and measure radon directly, and (ii) one-filter monitors (e.g. Stockburger and Sittkus, 1966; Paatero et al., 1998; Levin et al., 2002), which sample and measure radon progeny. Of the one-filter monitors, there are different designs, which target  $\alpha$  or  $\beta$  activity, with static, alternating, or moving filters. A third method for direct atmospheric  $^{222}\text{Rn}$  monitoring more recently applied at several sites in Spain (Grossi et al., 2012) as well as in the German Alps at Schneefernerhaus (Frank et al., 2016) monitors the activity of the radon progeny  $^{218}\text{Po}$  that is produced in situ by  $^{222}\text{Rn}$  decay in a detector chamber permanently flushed with sample air. In this chamber the positively charged  $^{218}\text{Po}$  atoms are accelerated in a high-voltage (e.g. 30 kV) field that is maintained between the chamber surface and a surface barrier detector for  $\alpha$  detection. As for the dual-flow-loop two-filter monitors, the sensitivity of this instrument type depends on the detector volume. If properly calibrated, monitors that sample  $^{222}\text{Rn}$  directly are principally more accurate than those which sample aerosol-bound  $^{222}\text{Rn}$  progeny, because no correction for disequilibrium is needed to estimate atmospheric  $^{222}\text{Rn}$  activity concentration.

Here we report on a recent extensive radon comparison project, conducted mainly in the framework of the European Infrastructure Project InGOS (<http://www.ingos-infrastructure.eu/>), across nine European measurement sites (Pallas and Helsinki, FI; Mace Head, IR; Lutjewad and Cabauw, NL; Gif-sur-Yvette, F; and Schauinsland, Hohenpeißenberg (HPB), and Heidelberg, DE). At all sites, the routine local  $^{222}\text{Rn}$  activity concentration measurements were compared to observations performed with the original (Levin et al., 2002) or a recently modernized (Rosenfeld, 2010) Heidelberg radon monitor (HRM). At stations where the two-filter technique is employed, i.e. Lutjewad (60 m a.g.l.), Cabauw (20 and 200 m a.g.l.), and Heidelberg (30 m a.g.l.), preliminary information about the mean height-dependent disequilibrium between  $^{222}\text{Rn}$  and its progeny can also be ob-

tained from the comparisons. Disequilibrium between  $^{222}\text{Rn}$  and its progeny in the atmosphere is generally largest close to the ground where soil-borne  $^{222}\text{Rn}$  gas exhales into the atmosphere but the short-lived progeny have not yet had sufficient time to reach radioactive equilibrium with  $^{222}\text{Rn}$ . The disequilibrium profile depends on the turbulent mixing conditions, particularly below 5–10 m a.g.l. (Jacobi and André, 1963). It may also occur through wet and dry deposition of the aerosol-bound progeny (Porstendörfer, 1994).  $^{222}\text{Rn}$  progeny loss may also occur when air is sampled through long tubing. This effect on measurements with the HRM is quantitatively investigated in the accompanying paper by Levin et al. (2017).

## 2 Methods

### 2.1 Australian Nuclear Science and Technology Organisation (ANSTO) two-filter monitors

The dual-flow-loop two-filter detectors employed within the European network were designed and built at the ANSTO, improving upon an earlier design by Thomas and Leclaire (1970). The first filter removes all ambient radon ( $^{222}\text{Rn}$ ) and thoron ( $^{220}\text{Rn}$ ) progeny from the airstream, which then passes into a large delay volume. Depending on the sampling height and flow rate, the volume of the intake system is adjusted to delay the airstream by 4–5 min to allow for decay of the short-lived isotope  $^{220}\text{Rn}$  ( $T_{1/2} = 56$  s). The rate of the first flow loop (which moves sample air through the detector) is set to exchange the delay volume's air in approximately 20 min, allowing new radon progeny to form. The rate of the second flow loop (which circulates air within the delay volume) is set so as to pass the entire volume of the delay chamber through the second filter (a low-impedance 625 mesh stainless steel screen) and a flow homogenizer about every 2 min, to make sure that all  $^{218}\text{Po}$  progeny ( $T_{1/2} = 3$  min) are collected. The newly formed unattached  $^{218}\text{Po}$  and  $^{214}\text{Po}$  are collected on the second filter and their  $\alpha$  decays are counted with a ZnS-photomultiplier system. Atmospheric  $^{222}\text{Rn}$  concentrations are then determined from the  $\alpha$  count rate and flow rate. The monitor's lower limit of detection varies primarily with the size of the detector volume, from  $\sim 0.25 \text{ Bq m}^{-3}$  (for a 100 L detector) to  $< 0.01 \text{ Bq m}^{-3}$  (for a 5000 L detector). Sample air is pushed (rather than sucked) through the detector, enabling the detector and associated plumbing to be kept at a slight overpressure compared to ambient air (+100 to +150 Pa) to minimize the chance of near-surface or indoor air contaminating observations, should small leaks develop in the system. At sites prone to heavy aerosol loading, a pre-filter is usually installed upstream of the inlet delay volume to protect the detector's primary filter and keep the intake line clean of Rn-producing aerosol. While two-filter detectors are well-suited to long-term, low-maintenance operation, they

are large (3 m) and have a slow (45 min) response time, which prevents them from being multiplexed on tall towers. In routine operation these monitors are calibrated monthly (which can be corrected for in post-processing; Griffiths et al., 2016) by injecting radon from a well-characterized (to ca.  $\pm 4\%$ ) Pylon  $^{226}\text{Ra}$  source at a flow rate of ca.  $80\text{ cc min}^{-1}$ . Instrumental background (zero count) checks are performed quarterly, from which a linear model of  $^{210}\text{Pb}$  ( $T_{1/2} = 22.3$  years) accumulation on the detector's second filter is derived and removed from the raw counts. Net counts are subsequently calibrated to atmospheric radon activity concentration.

## 2.2 One-filter $\alpha$ - or $\beta$ -activity monitors

One-filter detectors measure the decay rates of aerosol-bound  $^{222}\text{Rn}$  progeny directly accumulated by air filtration. Their  $\alpha$  and/or  $\beta$  activity is then measured in situ with dedicated detector systems. Since they normally consist of only a filter head, counting electronics, and a pumping device, they are much more compact than two-filter radon monitors. A disadvantage of the one-filter method, however, is that atmospheric  $^{222}\text{Rn}$  activity concentrations can only be determined by making assumptions about the radioactive disequilibrium between  $^{222}\text{Rn}$  and its measured progeny in the atmosphere. This disequilibrium changes with height above ground and the atmospheric mixing state (Jacobi and André, 1963). Furthermore, aerosol removal processes, such as dry or wet deposition, may bias the measurement. Depending on the location of the station and the meteorological conditions (atmospheric humidity and precipitation events), these latter effects may be as large as 30 % (e.g. Xia et al., 2010).

Also, one-filter detectors sample not only  $^{222}\text{Rn}$  progeny but also the aerosol-bound decay products of  $^{220}\text{Rn}$ . Although the activity concentrations of  $^{220}\text{Rn}$  itself are 1 to 2 orders of magnitude smaller than those of  $^{222}\text{Rn}$  in the continental atmosphere (Jacobi and André, 1963; Volpp, 1984), its long-lived progeny  $^{212}\text{Pb}$  ( $T_{1/2} = 10.6\text{ h}$ ) may accumulate on static filters. The  $\alpha$  activity of its progeny  $^{212}\text{Po}$  thus needs to be carefully separated, e.g. by spectroscopy, in such systems (see e.g. Levin et al., 2002, and Sect. 2.2.1.).

### 2.2.1 Heidelberg one-filter $\alpha$ monitor (HRM)

The original HRM was designed in the 1990s and is described in detail by Levin et al. (2002). Briefly, the system consists of a homemade filter holder carrying a Whatman quartz filter (QMA Ø 47 mm), which continuously collects all aerosols from an ambient airflow of ca.  $1\text{ m}^3\text{ h}^{-1}$ , monitored with a mass flow meter (Bronkhorst, model F-112AC-AAD-22-V). The face velocity is approximately  $0.15\text{ m s}^{-1}$  and the pressure drop over the filter about 5 kPa. Except for situations of very high ambient aerosol concentration, which could then block the filter, the filter is changed once per month. A surface barrier detector (Canberra CAM 900 mm<sup>2</sup> active surface) with pre-amplifier is mounted in the filter

holder about 5 mm from the loaded filter's surface to measure the  $\alpha$  particles from the decaying  $^{222}\text{Rn}$  and  $^{220}\text{Rn}$  progeny. Half-hourly integrated  $\alpha$ -spectra are stored and allow separation of the  $^{222}\text{Rn}$ -derived  $^{214}\text{Po}$  from the high energy  $^{220}\text{Rn}$ -derived  $^{212}\text{Po}$  counts. The methodology of separating  $^{218}\text{Po}$  and  $^{212}\text{Bi}$  counts from the spectra, and calculating the  $\alpha$  activity of  $^{214}\text{Po}$  on the filter, is explained in detail by Levin et al. (2002). From the flow rate through the filter the atmospheric  $^{214}\text{Po}$  activity concentration can be calculated, taking into account the filter efficiency and the solid angle of the detector (which depends on the distance of the detector from the filter).

In 2010 the original HRM design was modernized by implementing state-of-the-art electronics, data acquisition, and evaluation hardware and software (Rosenfeld, 2010). The filter holder was also slightly modified to allow more direct air flow from the intake onto the filter (avoiding potential loss of aerosols at the surfaces of the filter holder). Other aspects, however, including the solid angle of the detector and all other parameters, were kept the same. Long-term comparisons between a modernized HRM and our reference monitor that has been running at Heidelberg station since 1999 with regular checks of its measurement efficiency using a  $^{241}\text{Am}$  ( $^{241}\text{Am}$ )  $\alpha$  source showed no significant difference between the first- and the second-generation monitors (see also Sect. 2.3).

The HRM is not calibrated as such. Except for a calculation of the solid angle of the detector (solid angle = 0.265; Cuntz, 1997), we assume that the detector efficiency for  $\alpha$  particles is 100 %. The filter efficiency has been determined to be 100 %, except for the first few hours after filter change, when the aerosol loading is still very low. The mass flow meter has been calibrated by the company to within  $\pm 2\%$ . Atmospheric  $^{222}\text{Rn}$  activity concentrations can then be derived from atmospheric  $^{214}\text{Po}$  activity concentration, if the disequilibrium between  $^{222}\text{Rn}$  and its progeny at the measurement site is known (see below).

### 2.2.2 Finnish Meteorological Institute (FMI) one-filter $\beta$ -activity monitors

The FMI standard one-filter  $\beta$ -activity monitor in Helsinki is based on a pair of filter-holder/GM-tube assemblies, together with supporting electronics. Glass fiber filters (Whatman GF/A,  $130 \times 120\text{ mm}^2$ ) are placed around cylindrical filter holders with Geiger–Müller (GM) tubes inside (Paatero et al., 1994). Air is drawn through the filters alternately in 4 h periods at ca.  $23\text{ m}^3\text{ h}^{-1}$ , and counts from both GM counters are read and saved in 1 min intervals. Filters are changed every 1 to 2 weeks. The particle removal efficiency of the glass fiber filter was measured to be better than 99 % with a face velocity of  $0.10\text{ m s}^{-1}$  and a pressure drop of 6 kPa (Mattsson et al., 1965). The filter-holder/GM-tube assemblies are surrounded by lead shielding to reduce the back-

ground count rate.  $^{222}\text{Rn}$  activity concentration is calculated assuming (i) equilibrium between  $^{222}\text{Rn}$  and its short-lived progeny nuclides and (ii) there is no significant amount of long-lived beta activity (artificial or from  $^{212}\text{Pb}$  from the  $^{220}\text{Rn}$  series) present. The  $\beta$ -counting efficiencies are taken to be 0.96 % for  $^{214}\text{Pb}$  and 4.3 % for  $^{214}\text{Bi}$ , determined with an analyser utilizing an alpha-beta pseudo-coincidence technique (Mattsson et al., 1996). These counting efficiencies are used for both FMI systems at Pallas (FMI-1) and in Helsinki (FMI-2), as the counting geometries and GM-tube models are identical. This type of monitor was originally designed and employed in the early 1960s for radiation monitoring purposes; it was not specifically designed for  $^{222}\text{Rn}$  measurements.

### 2.2.3 LSCE active deposit moving filter progeny monitor

The LSCE monitor (Polian, 1986; Biraud, 2000) determines  $^{222}\text{Rn}$  activity from measurements of its short-lived progeny  $^{218}\text{Po}$  and  $^{214}\text{Po}$  and uses the so-called active deposit method with a moving filter tape. The measurement is a two-stage process with a sampling period, where attached radon progeny are collected on the cellulose filter (Pöllman-Schneider), followed by a counting period, which begins after the exposed portion of filter tape ( $13.8\text{ cm}^2$ ) has been advanced under the detector. Ambient air is pumped through the filter (deposition velocity ca.  $1\text{ m s}^{-1}$ ) for 2 h at a flow rate of about  $12\text{--}14\text{ m}^3\text{ h}^{-1}$ . Following this sampling period the filter tape advances under an  $\alpha$  spectrometer (scintillator from Harshaw Company and photomultiplier from EMI, Electronics Ltd) to measure the radioactive decay for 2 h. During this counting period, the radioactive decay of  $^{218}\text{Po}$ ,  $^{214}\text{Po}$  and  $^{212}\text{Po}$  (to determine the  $^{220}\text{Rn}$  activity) on the filter is logged every 10 min. Knowing the temporal evolution of the  $\alpha$  decays on the filter during the 2 h counting, atmospheric  $^{222}\text{Rn}$  (resp.  $^{222}\text{Rn}$  progeny) activity when the sample was being collected can be calculated (Biraud, 2000).

### 2.2.4 Bundesamt für Strahlenschutz $\alpha/\beta$ monitor (P3)

The Federal Office for Radiation Protection (BfS) developed the  $\alpha/\beta$  monitor (so-called P3) in the late 1950s to continuously monitor the natural ( $^{220}\text{Rn}/^{212}\text{Po}$  and  $^{222}\text{Rn}$ ) and artificial  $\beta$ -activity concentrations in ambient air. The technique applied is based on a static one-filter detection system (see Stockburger, 1960, and Stockburger and Sittkus, 1966, for details). The electronics for counting and data recording as well as the pumping system was modernized several times since 1966, but the detector system is still unchanged. Ambient air is drawn continuously with an airflow of ca.  $50\text{ m}^3\text{ h}^{-1}$  through a cellulose nitrate membrane filter (pore size  $1.2\text{ }\mu\text{m}$ , Sartorius Stedim Biotech). On this filter, aerosols, including the progeny of  $^{222}\text{Rn}$  and  $^{220}\text{Rn}$ , are quantitatively collected and the activities are measured with

a (custom-made) sandwich counter, consisting of three independent proportional gas flow counters (counting gas: 100 % methane 2.5). The exposed effective filter size is  $300\text{ cm}^2$  ( $0.23 \times 0.13\text{ m}^2$ ), the face velocity  $0.46\text{ m s}^{-1}$ , and the pressure drop ca. 22 kPa. The high voltages of the counters as well as the thickness of the foils between them are adjusted in such a way that the lower energy  $\alpha$  particles are measured by the first counter above the filter, the high-energy  $\alpha$  particles by the middle counter, and only the  $\beta$  particles are measured by the third counter. The  $\alpha$  activity of the short-lived  $^{222}\text{Rn}$  progeny  $^{218}\text{Po}$  ( $\alpha_E = 6.0\text{ MeV}$ ,  $T_{1/2} = 3.05\text{ min}$ ) and  $^{214}\text{Po}$  ( $\alpha_E = 7.69\text{ MeV}$ ,  $T_{1/2} = 164\text{ }\mu\text{s}$ ) collected on the filter is measured in situ, mainly by the counter positioned directly above the filter. Only the high-energy  $\alpha$  particles (8.78 MeV) from the decay of  $^{212}\text{Po}$  from the  $^{220}\text{Rn}$  decay chain could be measured in the middle proportional counters. Based on this count rate, corrections are made for activity contributions coming from the progeny of  $^{220}\text{Rn}$  to the ones of  $^{222}\text{Rn}$  measured by the lower counter. From this corrected count rate, the atmospheric  $^{222}\text{Rn}$  activity concentration is derived, assuming an equilibrium of  $^{222}\text{Rn}$  with the measured progeny. Finally, the artificial  $\beta$  activity is calculated.

### 2.2.5 Tracerlab Working Level Monitor (WLM) one-filter system

The Tracerlab WLM is a one-filter instrument (using a quantitatively collecting cellulose nitrate membrane filter, pore size  $0.8\text{ }\mu\text{m}$ , effective diameter 25 mm) that measures the potential  $\alpha$ -energy concentration (typically given in units of  $\text{J m}^{-3}$ , however, here as “radon equivalent” in  $\text{Bq m}^{-3}$ ). The monitor uses  $\alpha$  spectroscopy, so discrimination between  $^{218}\text{Po}$ ,  $^{214}\text{Po}$ , and also  $^{214}\text{Po}$  and  $^{212}\text{Po}$  is possible. The atmospheric  $^{222}\text{Rn}$  activity concentration is estimated using the ratio of three  $^{222}\text{Rn}$  progeny ( $^{218}\text{Po}$ ,  $^{214}\text{Po}$ ,  $^{214}\text{Pb}$ ) and the airflow (typical flow rate ca.  $0.7\text{ m}^3\text{ h}^{-1}$ , filter face velocity ca.  $0.4\text{ m s}^{-1}$ ) recorded by means of a mass flow controller, assuming equilibrium between  $^{222}\text{Rn}$  and its progeny. The WLM uses a mathematical calibration method. There is no explicit mathematical formula available because an iterative method is applied. The sampling and the decay of the filter activities are described by differential equations:

$$dA(^{218}\text{Po})/dt = C(^{218}\text{Po}) \cdot V - \lambda(^{218}\text{Po}) \cdot A(^{218}\text{Po})$$

$$dA(^{214}\text{Pb})/dt = C(^{214}\text{Pb}) \cdot V - \lambda(^{214}\text{Po}) \cdot (A(^{218}\text{Po}) - A(^{214}\text{Pb}))$$

$$dA(^{214}\text{Bi})/dt = C(^{214}\text{Bi}) \cdot V - \lambda(^{214}\text{Bi}) \cdot (A(^{214}\text{Pb}) - A(^{214}\text{Bi}))$$

$$dN(^{218}\text{Po})/dt = \eta \cdot A(^{218}\text{Po})$$

$$dN(^{214}\text{Po})/dt = \eta \cdot A(^{214}\text{Po}) \text{ with : } A(^{214}\text{Po}) = A(^{214}\text{Bi}),$$

where  $A$  represents filter activities of the Rn progeny,  $C$  is the activity concentration of the Rn progeny in air,  $V$  is the

online measured volume air flow rate,  $\lambda$  are the decay constants,  $N$  is the number of  $\alpha$  counts, and  $\eta$  is the counting efficiency of the detector-filter system.

The microcomputer of the WLM integrates in real time the differential equations for 20 different initial sets of the air activity concentrations  $C(^{218}\text{Po})$ ,  $C(^{214}\text{Pb})$ , and  $C(^{214}\text{Bi})$ . That is, the collection and the decay of the filter activity is simulated during the measurement. The result of the 20 simultaneous simulations are 20 pairs of calculated counts  $N(^{218}\text{Po})$  and  $N(^{214}\text{Pb})$ .

The used sets of air activities are distributed over the range from  $C(^{218}\text{Po}) : C(^{214}\text{Pb}) : C(^{214}\text{Bi}) = 26.34 : 1.862 : 0.132$  to  $C(^{218}\text{Po}) : C(^{214}\text{Pb}) : C(^{214}\text{Bi}) = 3.766 : 3.766 : 3.766$ . The calculated  $\alpha$  counts of  $^{218}\text{Po}$  and  $^{214}\text{Po}$  for each of the 20 sets are compared with the real  $\alpha$  counts seen by the detector. The ratio of the air activities, which fits best is taken to calculate the calibration factors for the potential  $\alpha$  energy and the Rn progeny. The activity concentration of  $^{218}\text{Po}$  and the concentration ratio  $^{218}\text{Po}$  and  $^{214}\text{Bi}$  are used to estimate the radon gas concentration at equilibrium according to

$$C(^{222}\text{Rn}) = C(^{218}\text{Po}) \cdot (C(^{218}\text{Po}) / C(^{214}\text{Bi})) \cdot k \text{ with } k = 0.3.$$

Cycle time is 1 h, and the filter is changed every 24 h. The manufacturer describes the detection limit of this instrument as  $0.2 \text{ Bq m}^{-3}$ , the uncertainty of measured activity with  $\pm 5\%$ , and the uncertainty of estimated  $^{222}\text{Rn}$  assuming equilibrium with  $\pm 25\%$ . (Method description from the operating manual of “Tracerlab WLM ASF 200” by TRACERLAB GmbH, Aachener Str. 1354, 50859 Cologne, Germany.)

### 2.3 Method of comparison between radon monitors

As an example of the comparison method used throughout this study, here we compare observations between an original HRM (i.e. our reference monitor, called HD-R (Heidelberg reference), that is used as reference throughout the comparison project to calibrate all other monitors that were sent to the various stations) and a modernized HRM in Heidelberg. A typical comparison period is displayed in Fig. 1. The upper panel of Fig. 1 shows the atmospheric  $^{214}\text{Po}$  activity concentrations measured over 6 weeks in spring 2012 with two Heidelberg monitors (HD-R and the first prototype of the modernized version called “1\_HD”). For a quantitative evaluation of the compatibility of measurements between the two monitors we first calculate the half-hourly activity ratios. The mean of these ratios (Fig. 1b) was  $1.012 \pm 0.127$  in the concentration range 1 to  $15 \text{ Bq m}^{-3}$ , which is typical for the Heidelberg measurement site, sampling air from about 30 m a.g.l. The half-hourly activity ratios show increasing scatter when ambient concentrations decrease. Linear regression of the half-hourly activity concentration data is displayed in Fig. 1c. The slope of the York fit (York et al., 2004), taking into account errors in both the  $x$  and  $y$  components, is  $1.021 \pm 0.016$ , i.e. not significantly different from unity

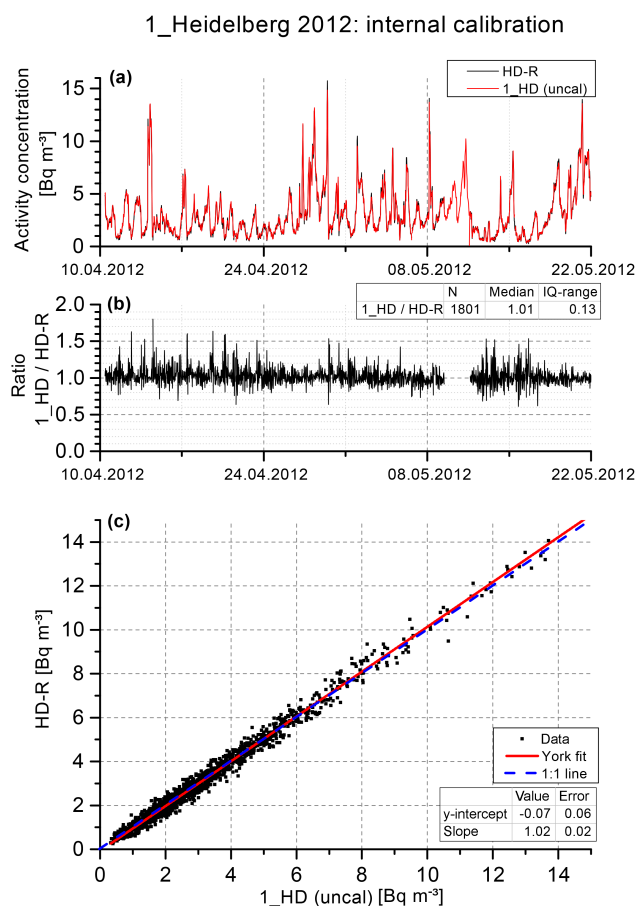


**Figure 1.** Comparison of  $^{214}\text{Po}$  activity concentrations of two Heidelberg radon monitors. HD-R is the monitor routinely running at the Heidelberg measurement site. 1\_HD (uncal) is a monitor which had not been calibrated with HD-R before. All monitors that were used for the comparison campaigns were calibrated against HD-R.

and the intercept is very close to zero. The uncertainty of the slope is very small and may be used as an approximation of the mean compatibility of long-term measurements with different Heidelberg instruments. Likewise, the standard deviation of the activity concentration ratios allows an estimate of the typical measurement repeatability in the concentration range at the observational site. The respective standard deviation of ca. 13 % for the half-hourly ratios of the two Heidelberg data sets from Fig. 1b is at the upper end of our monitor comparability (generally between 7 and 14 %). From this we can estimate a typical uncertainty of half-hourly atmospheric  $^{214}\text{Po}$  data of about 10 %. This is in accordance with uncertainty estimates reported by Levin et al. (2002).

Similar comparison evaluations to those shown in Fig. 1 were made for a pair of monitors at Heidelberg and for detector pairs (mobile HRMs and routine station monitors) at the other sites included in the European Radon Comparison Project. It should be noted that in all comparisons presented here (see Supplement Figs. S1–S12, Schmithüsen et



**Table 1.** Results from comparisons performed with the Heidelberg radon monitor (HRM) run at different European stations. The slopes (correction factors) are defined as (routine station monitor) / HRM (see Figs. S1 – S12).

ANSTO monitors	Period	Activity range	Slope	Offset
Cabauw: 200/180 m	10 July–26 August 2012	0–8 Bq m <sup>-3</sup>	1.11 ± 0.04	0.11 ± 0.06
Cabauw: 20 m	27 June 2012–10 January 2013	0–12 Bq m <sup>-3</sup>	1.30 ± 0.01	0.21 ± 0.03
Lutjewad: 60 m	1 January–1 October 2007	0–6 Bq m <sup>-3</sup>	1.11 ± 0.02	0.11 ± 0.02
Heidelberg: 35 m	25 April–31 July 2015	0–15 Bq m <sup>-3</sup>	1.22 ± 0.01	0.42 ± 0.04
Other monitors				
Pallas: FMI-1 2014	14 June–15 September 2014	0–6 Bq m <sup>-3</sup>	1.45 ± 0.05	0.18 ± 0.06
Helsinki: FMI-2 May 2014	22 May–10 June 2014	0–6 Bq m <sup>-3</sup>	1.04 ± 0.06	−0.03 ± 0.11
Helsinki: FMI-2 October 2014	1–22 October 2014	0–10 Bq m <sup>-3</sup>	1.02 ± 0.03	−0.03 ± 0.09
Mace Head: LSCE 2013	4 March–20 May 2013	0–3.5 Bq m <sup>-3</sup>	0.95 ± 0.07	−0.06 ± 0.06
GIF: LSCE 2014	27 February–28 April 2014	0–9 Bq m <sup>-3</sup>	0.68 ± 0.03	−0.18 ± 0.09
SIL: Bfs 2013 vs. 5_SIL2	24 September–10 December 2013	0–8 Bq m <sup>-3</sup>	1.12 ± 0.02	0.24 ± 0.04
SIL: Bfs 2013 vs. 9_InGOS	24 September–10 December 2013	0–8 Bq m <sup>-3</sup>	1.12 ± 0.02	0.24 ± 0.04
HPB: Tracerlab 2014	1 January 2014–30 April 2014	0–12 Bq m <sup>-3</sup>	1.03 ± 0.02	0.26 ± 0.05

**Figure 2.** Map of European stations where  $^{222}\text{Rn}$  comparison campaigns were conducted. This map was created with Google Earth (<http://earth.google.com>).

al., 2017), we do not correct for disequilibrium but directly compare the  $^{214}\text{Po}$  or other  $^{222}\text{Rn}$  progeny activity concentrations (in the case of one-filter systems) or to  $^{222}\text{Rn}$  activity concentrations (in the case of two-filter systems, i.e. from ANSTO).

## 2.4 Site descriptions and $^{222}\text{Rn}$ instrumentation at the comparison stations

Between 2007 and 2015, different HRMs were sent from Heidelberg to eight stations in Europe for comparison with the local radon measurement systems (for station locations, see map Fig. 2). In addition, comparison between the HRM and a newly installed ANSTO monitor in Heidelberg was made. Before and after each measurement campaign, the mobile HRM was calibrated against our original reference monitor HD-R in the Heidelberg laboratory. All comparison periods at the remote stations covered at least 4 weeks, to obtain sufficient data and sample different meteorological conditions. The stations, campaign dates, concentration ranges covered, as well as slopes and y intercepts of the regression lines are summarized in Table 1. A brief description of the station characteristics and routine measurement systems used at these sites is given in the following sections.

### 2.4.1 Pallas (FI, 67°58' N, 24°07' E; 565 m a.s.l.)

The WMO/GAW station Pallas is located in Northern Finland ca. 170 km north of the Arctic Circle. The station lies on top of a treeless subarctic hill (fell), Sammaltunturi, at an elevation of 565 m a.s.l., and some 200–300 m higher than the surrounding area. Routine radon measurements at this site are conducted using a simplified FMI  $\beta$ -activity monitor. This monitor has only one filter-holder/GM-tube assembly through which air is continuously drawn. This simplified monitor does not take into account possible beta activity from artificial (i.e. long-lived) radio nuclides or  $^{220}\text{Rn}$  progeny. It was adapted for Pallas because the station is not part of the national radiation surveillance network. Most of the year,  $^{220}\text{Rn}$  progeny cannot be transported from the local soil to the atmosphere due to frozen ground and snow cover. However,

at times of the year when local soils do emit  $^{220}\text{Rn}$  to the atmosphere it rarely influences observations since the station, due to its elevation, predominantly samples free tropospheric air. Therefore,  $^{220}\text{Rn}$  progeny have a negligible contribution to the total beta count rate (Mattsson et al., 1996; Paatero et al., 1998). For the same reason  $^{222}\text{Rn}$  and its short-lived progeny at this site predominantly arise through long-range transport and are consequently close to equilibrium during most meteorological situations (see below).

Ambient air is collected via an inlet 5 m a.g.l. Due to its elevation, the station is in cloud from time to time, ca. 10 % of the time during summer and up to 40 % of the time during autumn (Hatakka et al., 2003). For this reason the sampling line inlet is warmed during the seasons when the temperature can drop below freezing (ca. October–May). A rough estimation of the  $1\sigma$  counting statistics of the Pallas monitor is  $\pm 20\%$ , assuming a stable  $^{222}\text{Rn}$  activity concentration of  $1 \text{ Bq m}^{-3}$ . The comparison campaign at Pallas was conducted during summer and autumn, i.e. from 14 June to 15 September 2014. The activity concentration range covered during this campaign (as measured by the HRM) was between 0.05 and  $6 \text{ Bq m}^{-3}$ .

As with all systems that measure aerosol-bound  $^{222}\text{Rn}$  progeny, there are uncertainties associated with estimating atmospheric  $^{222}\text{Rn}$  activity concentration due to potential disequilibrium between  $^{222}\text{Rn}$  and its progeny. This is particularly the case when the air is humidity saturated. According to Gründel and Porstendörfer (2004) over 80 % of the short-lived radon progeny are attached to accumulation-mode particles. If the monitor is sampling in cloud or fog, these particles can form cloud droplets. Komppula et al. (2005) have reported that at Pallas on the average 87 % of the accumulation-mode particles and 30 % of Aitken-mode particles grow to cloud droplets. The system does not collect these droplets due to the sampling line design. However, the comparison at this station is between a pair of one-filter systems, and both instruments encounter this problem.

#### 2.4.2 Helsinki (FI, 60°12' N, 24°58' E; 26 m a.s.l.)

The FMI's head office is located on top of a small hill at Kumpula campus, Helsinki, about 4 km NNE of the city centre. Routine radon measurements are conducted using a standard FMI one-filter  $\beta$ -activity monitor. Ambient air is collected at 27 m a.g.l. The estimated counting uncertainty is  $\pm 20\%$ , assuming a stable  $^{222}\text{Rn}$  activity concentration of  $1 \text{ Bq m}^{-3}$ . The comparisons were conducted in two periods, i.e. from 22 May to 10 June and from 1 to 22 October 2014. The activity concentrations covered ranges in the first campaign from almost zero to  $6 \text{ Bq m}^{-3}$  and in the second campaign from almost 0 up to ca.  $10 \text{ Bq m}^{-3}$ .

#### 2.4.3 Mace Head (IR, 53°20' N, 9°54' W; 15 m a.s.l.)

The WMO/GAW and AGAGE station Mace Head is located at the west coast of Ireland, about 10 m away from the coastline (Fig. 2).  $^{222}\text{Rn}$  and  $^{220}\text{Rn}$  progeny have been monitored at Mace Head since June 1995. Routine measurements at this site are conducted using an active deposit moving-filter monitor, built and run by LSCE (Polian, 1986; Biraud, 2000). The detection limit of the LSCE measurement system is  $0.3 \text{ mBq m}^{-3}$ . The statistical error for a 2 h measurement period at ambient activity concentrations of about  $1 \text{ mBq m}^{-3}$  is close to 10 %, and the total error including uncertainties on flow rate and filtering efficiency is estimated to  $\pm 20\%$ .

The comparison measurements at Mace Head were made at the occasion of a comparison campaign performed for greenhouse gases measurements in the framework of the InGOS project (Vardag et al., 2014) from 4 March to 20 May 2013. Ambient air for  $^{222}\text{Rn}$  progeny comparison measurements was collected here using 11 m of standard Decarbon tubing (10 mm inner diameter) with the air intake at ca. 5 m a.g.l., the same height and type of tubing as for the routine measurements.

#### 2.4.4 Cabauw (NL, 51°58' N, 4°56' E; −0.7 m a.s.l.)

The instrument tower at Cabauw is 213 m high, built specifically for meteorological research to establish relations between the states of the atmospheric boundary layer, land surface conditions, and the general weather situation for all seasons. The tower is located in the western part of the Netherlands in a polder 0.7 m below average sea level. This site was chosen because it is representative for this part of the Netherlands. The North Sea is more than 50 km away to the WNW. Routine radon measurements at this site are conducted using two 1500 L ANSTO two-filter detectors operating at two heights: 20 and 200 m a.g.l. Air for each monitor is drawn at approximately  $6 \text{ m}^3 \text{ h}^{-1}$  through 7 cm outer diameter terylene fiber water pipes by a stack blower and pushed through the radon monitor.

Uncertainty of the calibrated hourly radon concentrations depends upon a combination of calibration source accuracy ( $\pm 4\%$  for both detectors), statistical counting error (which decreases with increasing radon activity concentration: e.g. 30 % at  $\sim 0.03 \text{ Bq m}^{-3}$ , 13 % at  $0.1 \text{ Bq m}^{-3}$ , 3 % at  $1 \text{ Bq m}^{-3}$ ), the coefficient of variability of valid monthly calibration coefficients (2.1 % at 20 m and 2.4 % at 200 m), and the background count variability ( $\sigma \approx 7 \text{ mBq m}^{-3}$ ). Therefore, at radon concentrations of around  $100 \text{ mBq m}^{-3}$ , the uncertainty would be of order 26 %, but this reduces to  $\sim 10\%$  at a concentration of  $1 \text{ Bq m}^{-3}$ .

As two ANSTO monitors are continuously analysing  $^{222}\text{Rn}$  in air from the 20 and the 200 m level at Cabauw, this provided the opportunity to compare both instruments with the HRM. Two Heidelberg radon monitors were used, and for some time they were run in parallel for comparisons at



both levels. However, as there was no possibility to install the HRM filter head directly at the 200 m level close to the ANSTO intake, it was set up at the 180 m platform, i.e. 20 m below the intake of the ANSTO system. This platform is accessible via stairs and/or an elevator, so that the HRM filter changes were easy to perform.

At Cabauw two tests could be conducted: (1) HRMa collected air directly at the 180 m level through a short (0.5 m) Teflon tubing (10 July–26 August 2012) and (2) HRMb collected air directly from the 20 m level also through a short (0.5 m) Teflon intake line (27 June 2012–10 January 2013).

#### 2.4.5 Lutjewad (NL, 53°24' N, 6°21' E; 1 m a.s.l.)

Lutjewad station is located directly on the sea dike at the Dutch North Sea coast in the so-called Julianapolder reclaimed in 1923. The location allows for the sampling of continental air masses with southerly winds, as well as nearly undisturbed marine air masses with a long North Sea fetch from the north.

Routine radon measurements at Lutjewad have been conducted since August 2005, using a 1500 L ANSTO two-filter monitor located in the Lutjewad station building. Sample air is drawn at a flow rate of  $4.8 \text{ m}^3 \text{ h}^{-1}$  from the top of a 60 m tower through 100 m of 100 mm internal diameter PVC pipe (van der Laan et al., 2010). As for the Cabauw monitors, the uncertainty of calibrated radon concentrations is a combination of source accuracy ( $\pm 4\%$ ), the detector's counting error (which decreases with increasing radon concentration, i.e. 30 % at  $0.04 \text{ Bq m}^{-3}$ , 15 % at  $0.1 \text{ Bq m}^{-3}$ , 3.5 % at  $1 \text{ Bq m}^{-3}$ ), the coefficient of variability of valid monthly calibration coefficients (2 %), and the background count variability ( $\sigma \approx 10 \text{ mBq m}^{-3}$ ). Therefore, at concentrations of around  $100 \text{ mBq m}^{-3}$ , the uncertainty would be of order 31 %, but this reduces to around 11 % at a concentration of  $1 \text{ Bq m}^{-3}$ .

For the comparison campaign at Lutjewad, the filter holder of the HRM was mounted also at the 60 m level of the tower with a 0.5 m Teflon inlet pipe and a funnel to prevent rainwater intake. The comparison was conducted from 1 January to 1 October 2007.

#### 2.4.6 Heidelberg (DE, 49°25' N, 8°41' E; 116 m a.s.l.)

Heidelberg is a medium size city located in the Upper Rhine valley in south-west Germany. Monitoring of air constituents such as greenhouse gases (Levin et al., 2011) is conducted from the roof of the institute's building on the university campus.  $^{222}\text{Rn}$  has been measured at this station since 1999 with an original HRM. Since April 2015 radon has also been monitored simultaneously with an ANSTO 1500 L two-filter radon monitor and a second HRM. Both detectors sample from a height of ca. 35 m a.g.l., through short co-located intake lines. The ANSTO monitor samples at a flow rate of ca.  $3 \text{ m}^3 \text{ h}^{-1}$ .

As for the Cabauw detector, the two-filter monitor at Heidelberg is calibrated at about monthly intervals by introducing an air stream with  $^{222}\text{Rn}$  from a  $^{226}\text{Ra}$  calibration source of known emission rate (Pylon model 2000A passive radon source). Background measurements are performed about every 3 months. Uncertainty of the calibrated hourly radon concentrations depends upon a combination of calibration source accuracy ( $\pm 4\%$ ), statistical counting error (which decreases with increasing radon concentration: e.g. 30 % at  $\sim 0.034 \text{ Bq m}^{-3}$ , 13 % at  $0.1 \text{ Bq m}^{-3}$ , 3.2 % at  $1 \text{ Bq m}^{-3}$ ), the coefficient of variability of valid monthly calibration coefficients (3.5 %), and the background count variability ( $\sigma \approx 5 \text{ mBq m}^{-3}$ ). Therefore, at radon concentrations of around  $100 \text{ mBq m}^{-3}$ , the uncertainty would be of order 26 %, but this reduces to  $\sim 11\%$  at a concentration of  $1 \text{ Bq m}^{-3}$ . The results from the HRM–ANSTO comparison in Heidelberg are presented for the period May–July 2015.

#### 2.4.7 Gif-sur-Yvette (F, 48°25' N, 02°05' E; 167 m a.s.l.)

Gif-sur-Yvette station is located approximately 20 km southwest of Paris. Routine radon measurements have been performed at this station since 2002 using an LSCE active deposit moving filter detector. However, unlike the LSCE monitor configuration at Mace Head, the sampling period at this site lasts only 1 h before the filter is placed under an  $\alpha$  spectrometer to measure the radioactive decay of the  $^{222}\text{Rn}$  and  $^{220}\text{Rn}$  progeny. The inlet line at Gif-sur-Yvette station is located only 2 m a.g.l., where the short-lived  $^{222}\text{Rn}$  progeny are not in equilibrium with the gaseous  $^{222}\text{Rn}$ . However, as we compare only  $^{214}\text{Po}$  activity concentrations, this is not relevant here. The comparison campaign at Gif-sur-Yvette was conducted from 27 February to 28 April 2014, with an activity concentration range of about  $0\text{--}9 \text{ Bq m}^{-3}$ .

#### 2.4.8 Schauinsland (DE, 47°55' N, 07°54' E; 1205 m a.s.l.)

The measurement station of BfS at Schauinsland in the Black Forest in south-western Germany is located on a mountain ridge at an elevation of about 1000 m above the Upper Rhine Valley. During daytime in summer the station is frequently influenced by upslope winds, while at night, and also in winter, it is often isolated from the valley meteorology by an inversion layer and samples free tropospheric air. Routine radon measurements are conducted at Schauinsland by the BfS using the P3  $\alpha/\beta$  monitor. Ambient air is drawn in continuously from ca. 2.5 m a.g.l. and pumped through the membrane filter (mixed cellulose ester,  $1.2 \mu\text{m}$ ,  $250 \times 150 \text{ mm}^2$  ME 28, Schleicher & Schuell, until April 2010; afterwards cellulose nitrate filters from Sartorius Stedim Biotech GmbH) for 1 week. After this sampling time the pump is switched off, a 1 h calibration check is performed using a  $^{241}\text{Am}/^{90}\text{Sr}$  source, the filter is replaced with a new one, the background is measured with a new

filter for an additional hour, and then the air flow is started again. The sensitivity for  $^{222}\text{Rn}$  is  $3.367 \text{ Bq cps}^{-1}$  (counts per second) or  $0.0673 \text{ Bq m}^{-3} \text{ cps}^{-1}$  for an airflow rate of about  $50 \text{ m}^3 \text{ h}^{-1}$ . The background count rate used for data evaluation is  $0.043 \text{ cps}$  and was determined during a period of several days with no airflow. The temporal resolution of  $^{222}\text{Rn}$  and progeny measurements is 10 min. Stockburger (1960) estimated an uncertainty of 3–4 % for a typical  $^{222}\text{Rn}$  measurement at Schauinsland at activity concentrations of  $1\text{--}4 \text{ Bq m}^{-3}$  (not taking into account uncertainties in the disequilibrium). More realistically, we assume an overall uncertainty (of  $^{214}\text{Po}$ ) to be comparable to that of the Heidelberg system, i.e. around 5–10 % for the activity concentration range of  $0\text{--}8 \text{ Bq m}^{-3}$ , as measured during the comparison of the two detection systems.

At Schauinsland, comparison with two HRMs was conducted in parallel from 24 September to 10 December 2013. An earlier comparison study with an ANSTO system had been performed in 2007–2008 by Xia et al. (2010). For this comparison the authors reported mean ratios between the ANSTO and the BfS system of  $\text{BfS} / \text{ANSTO} = 0.74$  to  $0.87$ , depending on meteorological conditions. Still, during dry weather situations with potentially small aerosol loss processes being active, the ANSTO system was measuring at least 14 % higher activity concentrations than the BfS system. We will discuss the results from this study to evaluate possible calibration differences between the one-filter systems and the ANSTO detectors, as well as for estimating  $^{214}\text{Po} / ^{222}\text{Rn}$  disequilibrium at the Schauinsland station.

#### 2.4.9 Hohenpeißenberg (DE, $47^\circ 48' \text{ N}$ , $11^\circ 01' \text{ E}$ ; 985 m a.s.l.)

The GAW station HPB is located on a small mountain ridge in the pre-Alps in southern Germany. It is run by the German Weather Service (DWD). Radon progeny measurements started here in 1999 with the data being available at WMO/GAW World Data Centre for Greenhouse Gases (WDCGG) (<http://ds.data.jma.go.jp/gmd/wdcgg/cgi-bin/wdcgg/accessdata.cgi?index=HPB647N00-DWD&para=222Rn&select=inventory>).

Routine radon measurements at this station are made using a Tracerlab WML monitor. The inlet line for the HPB  $^{222}\text{Rn}$  monitor consists of a ca. 0.4 m, 6 cm inner diameter PVC tubing. For comparison measurements with the HRM its 0.4 m long PFA tubing was mounted inside the HPB PVC tubing, ensuring the same air is sucked into the respective instruments. Both monitors were located at the HPB-GAW lab on the fourth floor of the building with the air intake directly at the window, ca. 10 m a.g.l. As no disequilibrium between atmospheric  $^{222}\text{Rn}$  and  $^{214}\text{Po}$  is taken into account in the data evaluation, we assume equal activity concentration of  $^{214}\text{Po}$  and estimated  $^{222}\text{Rn}$  of the Tracerlab WML detector in our comparison.

The last calibration of this instrument took place at the BfS, Berlin, Germany, with calibration mark 612/D-K-15063-01-00/2013-03 in March 2012 at activity concentrations measured by the reference monitor with  $10.1 \times 10^{-6} \text{ J m}^{-3}$  with an extended uncertainty of  $1.2 \times 10^{-6} \text{ J m}^{-3}$ . The HPB Tracerlab WLM measured an activity of  $9.2 \times 10^{-6} \text{ J m}^{-3}$  with an extended uncertainty of  $1.4 \times 10^{-6} \text{ J m}^{-3}$ , leading to a ratio between reference and examinee analyser of  $1.09 \pm 0.21$  on the 95 % confidence level. The comparison campaign with the HRM at HPB observatory was conducted from 1 January to 30 April 2014.

## 3 Results

### 3.1 Comparison at stations using two-filter ANSTO systems

#### 3.1.1 Results from 180 and 20 m at Cabauw

From 10 July to 26 August 2012 a HRM was installed on the Cabauw tower at 180 m, so that measurements could be conducted in parallel to the ANSTO system (collecting air from the 200 m level) without additional tubing. The results obtained from the available measurements are shown in Supplementary Fig. S1. The data cover a concentration range from close to zero up to  $8 \text{ Bq m}^{-3}$ , which is typical for this site and elevation. A short period of observations from 3 August 2012, directly after a filter change of the HRM, has been flagged; all other data were used for a linear regression. The correlation of the two data sets in Fig. S1, lower panel, yielded a slope of  $\text{ANSTO} / \text{HRM} = 1.11 \pm 0.04$ , i.e. on average the Cabauw ANSTO monitor at 200 m measured 11 % higher  $^{222}\text{Rn}$  activity concentrations than the  $^{214}\text{Po}$  activity concentration measured with the HRM at 180 m.

A second HRM was installed at 20 m on the Cabauw tower and measurements were conducted from 27 June 2012 until 10 January 2013 (Fig. S2). The activity concentrations covered by these measurements range from close to zero up to  $15 \text{ Bq m}^{-3}$ . Data from a few hours have been flagged as obvious outliers, but the remaining measurements yielded a slope of  $\text{ANSTO} / \text{HRM} = 1.30 \pm 0.01$  (Fig. S2, lower panel), i.e. on average the ANSTO monitor measured almost 30 % higher  $^{222}\text{Rn}$  activity concentrations at the 20 m level than  $^{214}\text{Po}$  activities measured with the HRM. At all height levels (even at 180 m a.g.l.) the  $^{214}\text{Po}$  activity concentrations measured with the HRM may not have been in full radioactive equilibrium with atmospheric  $^{222}\text{Rn}$ . As this disequilibrium is expected to increase with decreasing height above ground (Jacobi and André, 1963), a larger difference between the ANSTO and HRM monitors is expected at 20 compared to 180 m. However, part of the differences between the HRM and ANSTO systems at both levels may also be due to calibration differences between these two measurements systems (see Sect. 4.1).

### 3.1.2 Results from 60 m above ground at Lutjewad

An original HRM was installed and operated at Lutjewad from January to September 2007. For this comparison, the HRM filter head was mounted very close to the inlet of the ANSTO system on top of the tower at 60 m a.g.l., so that direct comparison of the data (without additional tubing) was possible. The comparison data are displayed in Fig. S3. The activity concentration range as measured with the ANSTO system was from close to 0 up to  $6 \text{ Bq m}^{-3}$ . The slope of the regression of all data yielded a mean of  $\text{ANSTO} / \text{HRM} = 1.11 \pm 0.02$ , i.e. the same value as observed at the 180 m level at Cabauw. Jacobi and André (1963) do not estimate changes of the disequilibrium between  $^{214}\text{Po}$  and  $^{222}\text{Rn}$  of more than a few percent for altitudes above 50 m a.g.l. This may indicate that the differences between the ANSTO and the HRM systems at Cabauw (180 m) and Lutjewad (60 m) are rather due to calibration differences than due to disequilibrium effects. We will discuss this point further in Sect. 4.1.

### 3.1.3 Results from 35 m above ground in Heidelberg

Comparison of results from the HRM and ANSTO systems run in Heidelberg since April 2015 is displayed in Fig. S4. Activity concentrations at this site and elevation ranged from almost 0 to about  $15 \text{ Bq m}^{-3}$ . The slope of the regression line of all half-hourly values was  $\text{ANSTO} / \text{HRM} = 1.22 \pm 0.01$ . As expected, the  $\text{ANSTO} / \text{HRM}$  ratio and thus the disequilibrium in Heidelberg for 35 m a.g.l. is slightly smaller than the one measured at Cabauw tower at the 20 m level.

## 3.2 Comparison at stations using one-filter systems

As described in Sect. 2.3, all other monitors compared in this study were essentially one-filter systems, i.e. they measured aerosol-bound  $^{222}\text{Rn}$  progeny to estimate atmospheric  $^{222}\text{Rn}$  activity concentration. For these stations, we either directly compare the  $^{214}\text{Po}$  activity concentrations or assume equilibrium between the estimated  $^{222}\text{Rn}$  from the station instrument, which we call “equivalent radon” in Figs. S5–S9 and the  $^{214}\text{Po}$  measurements of the HRM, as both systems suffer from similar aerosol loss processes. All comparison results are plotted in Supplementary Figs. S5–S12, while the slopes and offsets of the standard regression lines are listed in Table 1.

The range of regression slopes (routine station monitor/HRM) was between 0.68 and 1.45, while the offsets were generally small ( $-0.18 \dots +0.42 \text{ Bq m}^{-3}$ ). The huge range of slopes (i.e. differences in measurement principle or calibration of the different systems) underlines the importance of our radon comparison project. At some stations, a number of earlier comparison campaigns had been conducted (i.e. Schauinsland and Gif-sur Yvette) which showed slightly different slopes and offsets than listed in Table 1. However, we will not discuss these earlier comparison data here be-

cause the current study was conducted with HRM systems that were very well and consistently calibrated against the HD-R.

## 4 Discussion

### 4.1 Calibration differences

The comparison of one-filter monitors yields correction factors that allow normalizing  $^{214}\text{Po}$  or other  $^{222}\text{Rn}$  progeny-based  $^{222}\text{Rn}$  activity concentration measurements from a network of stations (e.g. for modelling studies). These normalized  $^{222}\text{Rn}$  data cannot be merged with true  $^{222}\text{Rn}$  data from two-filter systems without correcting them for disequilibrium. However, separating observed differences between HRM and two-filter systems, as obtained in our study, into a calibration and a disequilibrium part is not straightforward. The difficulty mainly comes from the fact that there is no common calibration method available that would serve both measurement systems.

All ANSTO monitors are calibrated with  $^{226}\text{Ra}$  sources that are certified as accurate to about 4 %. There are additional sources of error in the ANSTO  $^{222}\text{Rn}$  measurements, i.e. in the characterization of the instrumental background, flow rate stability, counting error, and calibration factor variability that, combined, result in an uncertainty for a 1 h concentration measurement of order 10 % at activity concentrations of  $\sim 1 \text{ Bq m}^{-3}$ . This uncertainty reduces for longer averaging times. Levin et al. (2002) have estimated a typical measurement uncertainty of the HRM for atmospheric  $^{214}\text{Po}$  activity concentrations for continental air to less than 10 %. This includes uncertainty of the flow rate, the counting statistics, and filter efficiency, solid angle of the detector, and uncertainty in the assumption of 100 % counting efficiency of the surface barrier detector for  $\alpha$  particles. The potential systematic bias of the HRM is, however, most probably smaller than 10 %, so that the maximum calibration bias between the two measurement systems (at full equilibrium between  $^{214}\text{Po}$  and  $^{222}\text{Rn}$ ) may be 12–15 %.

The only one-filter monitor included in our comparison study that had been externally calibrated was the Tracerlab WLM instrument running at HPB. Its calibration yielded a 9 % lower value compared to the reference at the calibration institution (see Sect. 2.4.9). When conducting the comparison campaign at HPB, the Tracerlab WLM system measured 3 % higher values than the HRM. This indicates that the HRM may measure  $^{214}\text{Po}$  activity concentrations too low by as much as 12 %, compared to the calibration unit at BfS in Berlin, Germany.

In fact, a calibration bias of about 12 % between the HRM and the ANSTO system would be in line with the measured 11 % differences found at the 180 m level at Cabauw and the 60 m level at Lutjewad. Then we would assume that the disequilibrium between  $^{214}\text{Po}$  (as measured with the HRM) and

**Table 2.** Estimated disequilibrium of Rn progeny measurements at the European monitoring stations where one-filter measurement systems are used (column 3), intercomparison factor (column 4, same as slopes listed in Table 1), and total (multiplicative) correction factors for  $^{222}\text{Rn}$  or progeny-based  $^{222}\text{Rn}$  measurements to bring them on the UHEI  $^{222}\text{Rn}$  scale (column 5) or on the ANSTO  $^{222}\text{Rn}$  scale (column 6).

Station	Type	$^{214}\text{Po} / ^{222}\text{Rn}$ disequilibrium factor	Comparison factor relative to UHEI $^{214}\text{Po}$ scale	Total correction factor UHEI $^{222}\text{Rn}$ scale	Total correction factor ANSTO $^{222}\text{Rn}$ scale
Pallas	progeny	0.85	1.45	0.81	0.90
Helsinki	progeny	0.90	1.04	1.07	1.19
Mace Head	progeny	1.00	0.95	1.05	1.17
Cabauw (20 and 180 m)	ANSTO	not appl.	not appl.	0.90	1.00
Lutjewad	ANSTO	not appl.	not appl.	0.90	1.00
Gif-sur-Yvette	progeny		0.68		
Schauinsland	progeny	0.80	1.12	1.12	1.24
Heidelberg	progeny	0.91	1.00	1.11	1.22
Hohenpeißenberg	progeny	0.85	1.03	1.14	1.27

$^{222}\text{Rn}$  (as measured with the ANSTO systems) is negligible above about 50 m a.g.l., which is supported by the theoretical estimates of Jacobi and André (1963). If the measured difference between ANSTO and HRM at 180 m at Cabauw would still include a contribution from disequilibrium, we would expect significant differences of the ANSTO / HRM ratio during stable and unstable atmospheric situations, with a higher ratio at unstable well-mixed atmospheric situations (i.e. during day) and a lower ratio during stable conditions (i.e. during night). With this in mind we evaluated these two situations separately but found no significant difference in results. Based on these independent findings, for the following discussion and estimate of disequilibrium factors, we thus do assume a calibration difference between ANSTO and HRM of 11 % (with an uncertainty of about 2–4 %).

#### 4.2 Preliminary estimate of $^{214}\text{Po} / ^{222}\text{Rn}$ disequilibria for European sites with one-filter systems

Taking into account the calibration bias,  $\text{ANSTO} / \text{HRM} = 1.11$ , we estimate a disequilibrium of  $^{214}\text{Po} / ^{222}\text{Rn} = 1.11 / 1.3 = 0.85$  for the 20 m level at Cabauw, where the measured slope  $\text{ANSTO} / \text{HRM}$  was 1.30 (Fig. S2). The uncertainty of this estimate is of order 10 %. A slightly higher disequilibrium value is estimated for Heidelberg (i.e.  $1.11 / 1.22 = 0.91$ , Table 2, third column). Cuntz (1997) determined a mean disequilibrium of  $0.704 \pm 0.081$  at the earlier Heidelberg sampling site at ca. 20 m a.g.l., based on a comparison with slow-pulse ionization chamber measurements. This earlier value is significantly smaller than our new estimate for 35 m a.g.l., based on the comparison with the Heidelberg ANSTO detector. However, if we take into account that the HRM is most probably measuring  $^{214}\text{Po}$  activity concentrations by 11 % too low we may attribute part of the earlier difference measured by Cuntz (1997) to a “calibration bias” of the

HRM; this would bring both disequilibrium values closer together.

Also, for all other European stations that were part of the comparison study using one-filter systems, average local disequilibrium factors need to be estimated before these data can be used for quantitative applications. We, therefore, made a respective preliminary attempt, based on the assumption that the  $^{214}\text{Po} / ^{222}\text{Rn}$  disequilibrium at non-coastal sites increases with decreasing height above local ground (Jacobi and André, 1963). For Helsinki, where sampling is conducted ca. 30 m a.g.l., we can assume a similar value as for Heidelberg 35 m a.g.l., i.e. about 0.9 (Table 2, third column). At Mace Head, located directly on the Irish coast, we can probably assume that the disequilibrium is similar to that at the coastal site Lutjewad (i.e. close to 1 or slightly lower, if the air has recently been in contact with land), despite sampling at Mace Head being conducted only from 5 m a.g.l. Only at the more continental station Gif-sur-Yvette, where air for  $^{222}\text{Rn}$  progeny measurements is sampled very close to the ground (i.e. 2 m), are we not able to make a justifiable disequilibrium estimate with the existing information.

In order to estimate an average disequilibrium value for the mountain sites Schauinsland, Hohenpeißenberg, and Pallas, we utilize results from the comparison campaign conducted between the BfS and ANSTO systems at Schauinsland (Xia et al., 2010). Their reported slopes of  $^{214}\text{Po}$  (BfS) /  $^{222}\text{Rn}$  (ANSTO) between 0.74 and 0.87 (from which we estimate a mean of 0.81) can be transferred to an ANSTO / HRM slope of 1.38, taking into account our mean comparison value of  $\text{BfS} / \text{HRM} = 1.12 \pm 0.02$  (Table 1). Then including the bias correction of 1.11 between ANSTO and HRM would yield a mean disequilibrium value of 0.8 for the Schauinsland mountain station (1205 m a.s.l.) where the air is collected from an inlet about 2.5 m a.g.l. This number is slightly smaller but still well in accordance with an earlier estimate from Cuntz (1997) of  $0.85 \pm 0.05$ . The mean disequilibrium values at Pallas and Hohenpeißenberg are probably

similar to Schauinsland or slightly larger (i.e. between 0.8 and 0.9), also because the air intake heights at these stations are slightly higher above local ground (between 5 and 10 m a.g.l.).

All our first estimates of mean disequilibrium factors for European stations with one-filter systems are listed in Table 2 (third column). They should be taken as preliminary, with a likely uncertainty (and variability due to different meteorological conditions) of about 0.05 to 0.1. We investigated the variation of monthly mean disequilibrium factors for Lutjewad and Heidelberg (Capuana, 2016), which were surprisingly constant with standard deviations smaller than 0.1 at both sites. Similar moderate variations were observed on the diurnal timescale with slightly lower (0.1) values during daytime in summer than during early morning. This finding is in accordance with earlier work reported by Porstendörfer (1994). Only during rare situations with fog at Lutjewad did we experience exceptional  $^{222}\text{Rn}$  progeny loss; otherwise, no systematic relation between disequilibrium and meteorological conditions was identified in our data sets. However, individual hourly measurements may show larger deviations from the averages given in Table 2. If we want to correct all European station data to be comparable with HRM  $^{222}\text{Rn}$  data (we call this here “UHEI  $^{222}\text{Rn}$  scale”), we have to combine two correction factors, the comparison factor from Table 1 (column 4 in Table 2) and the disequilibrium factor (column 3 in Table 2) for one-filter systems. This will yield  $^{222}\text{Rn}$  (UHEI  $^{222}\text{Rn}$  scale) = measured activity concentration / (comparison factor  $\times$  disequilibrium factor). If the data shall be normalized to the ANSTO scale, further multiplication of these values by 1.11 is required. Both total correction factors are listed in Table 2 (last two columns).

## 5 Conclusions

Our  $^{222}\text{Rn}$  comparison exercise has been very successful in providing correction factors to make European  $^{222}\text{Rn}$  and  $^{222}\text{Rn}$  progeny-based measurements comparable. The slopes given in Table 1 can be used to transfer data sets to the Heidelberg  $^{214}\text{Po}$  scale. In the case of one-filter systems, which measure only  $^{222}\text{Rn}$  progeny activity concentrations, further disequilibrium corrections are necessary to estimate atmospheric  $^{222}\text{Rn}$  activity concentrations. First preliminary estimates of average correction factors, based on comparisons between the one-filter HRM and the two-filter ANSTO systems at Cabauw, Lutjewad, Heidelberg, and Schauinsland range from 0.8 to 0.9. For model intercomparison studies, both corrections have to be applied to one-filter systems; therefore also the total multiplicative correction factors are presented (last two columns of Table 2). Further comparison studies, e.g. with ANSTO monitors or other measurement systems, are needed to better determine the disequilibrium between  $^{214}\text{Po}$  (and other  $^{222}\text{Rn}$  progeny) and  $^{222}\text{Rn}$  for the sites with one-filter systems, so that the one-filter-based

$^{222}\text{Rn}$  data can reliably be used for quantitative model comparison and flux estimates, e.g. using the radon tracer method (Levin et al., 1999).

*Data availability.* Data related to this paper are available online from the University of Heidelberg under doi:10.11588/data/10098.

**The Supplement related to this article is available online at doi:10.5194/amt-10-1299-2017-supplement.**

*Competing interests.* The authors declare that they have no conflict of interest.

*Acknowledgements.* The research leading to these results has received funding from the European Community's Seventh Framework Programme (FP7/2007-2013) in the InGOS project under grant agreement no. 284274. We wish to thank the technicians and personnel at the stations for their support during the comparison study and Martina Schmidt (Laboratoire des Science du Climat et de l'Environnement, CNRS/CEA, Gif-sur-Yvette, France) for organizational help during the comparison at Gif-sur-Yvette. John Moncrieff (University of Edinburgh) is gratefully acknowledged for donating his ANSTO monitor to Heidelberg University. We wish to thank Claudia Grossi and two anonymous reviewers for their helpful comments on our manuscript. Finally, we acknowledge financial support by Deutsche Forschungsgemeinschaft and Ruprecht-Karls-Universität Heidelberg within the funding programme Open Access Publishing.

Edited by: C. Brümmer

Reviewed by: C. Grossi and two anonymous referees

## References

- Biraud, S.: Vers la régionalisation des puits et sources des composés à effet de serre: analyse de la variabilité synoptique à l'observatoire de Mace Head, Irlande, PhD Thesis, University of Paris VII, France, 2000.
- Capuana, C.-A.: Calibration of ionization chambers and comparison of two monitors for radon measurement, BA Thesis, Institut für Umweltphysik, Heidelberg University, 2016 (in German).
- Chambers, S., Williams, A. G., Zahorowski, W., Griffiths, A. D., and Crawford, J.: Separating remote fetch and local mixing influences on vertical radon measurements in the lower atmosphere, *Tellus B*, 63, 843–859, 2011.
- Cuntz, M.: The Heidelberg  $^{222}\text{Rn}$  monitor: Calibration, optimisation, application, Diploma Thesis, Institut für Umweltphysik, Heidelberg University, Germany, 1997.
- Dörr, H., Kromer, B., Levin, I., Münnich, K. O., and Volpp, H. J.:  $\text{CO}_2$  and Radon-222 as tracers for atmospheric transport, *J. Geophys. Res.*, 88, 1309–1313, 1983.
- Frank, G., Salvamoser, J., and Steinkopf, T.: Messung radioaktiver Spurenstoffe in der Atmosphäre im Rahmen des

- Global Atmosphere Watch Programmes der WMO, Umweltforschungsstation Schneefernerhaus, Wissenschaftliche Resultate 2011/2012, [http://www.schneefernerhaus.de/fileadmin/web\\_data/bilder/pdf/UFS-Broschuere\\_2012.pdf](http://www.schneefernerhaus.de/fileadmin/web_data/bilder/pdf/UFS-Broschuere_2012.pdf), last access: 18 August, 2016.
- Griffiths, A. D., Chambers, S. D., Williams, A. G., and Werczynski, S.: Increasing the accuracy and temporal resolution of two-filter radon-222 measurements by correcting for the instrument response, *Atmos. Meas. Tech.*, 9, 2689–2707, doi:10.5194/amt-9-2689-2016, 2016.
- Grossi, C., Arnold, D., Adame, A. J., Lopez-Coto, I., Bolivar, J. P., de la Morena, B. A., and Vargas, A.: Atmospheric  $^{222}\text{Rn}$  concentration and source term at El Arenosillo 100 m meteorological tower in southwest, Spain, *Radiat. Meas.*, 47, 149–162, doi:10.1016/j.radmeas.2011.11.006, 2012.
- Gründel, M. and Porstendörfer, J.: Differences between the activity size distributions of the different natural radionuclide aerosols in outdoor air, *Atmos. Environ.*, 38, 3723–3728, 2004.
- Hatakka, J., Aalto, T., Aaltonen, V., Aurela, M., Hakola, H., Komppula, M., Laurila, T., Lihavainen, H., Paatero, J., Salminen, K., and Viisanen, Y.: Overview of the atmospheric research activities and results at Pallas GAW station, *Boreal Env. Res.*, 8, 365–383, 2003.
- Jacob, D. J. and Prather, M. J.: Radon-222 as a test of convective transport in a general circulation model, *Tellus B*, 42, 118–134, 1990.
- Jacob, D. J., Prather, M. J., Rasch, P. J., Shia R. L., Balkanski, Y., J., Beagley, S. R., Bergmann, D. J., Blackshear, W. T., Brown, M., Chiba, M., Chipperfield, M. P., Degrandpre, J., Dignon, J. E., Feichter, J., Genthon, C., Grose, W. L., Kasibhatla, P. S., Kohler, I., Kritz, M. A., Law, K., Penner, J. E., Ramonet, M., Reeves, C. E., Rotman, D. A., Stockwell, D. Z., Vanvelthoven, P. F. J., Verver, G., Wild, O., Yang, H., and Zimmermann, P.: Evaluation and intercomparison of global atmospheric transport models using Rn-222 and other short-lived tracers, *J. Geophys. Res.*, 102, 5953–5970, 1997.
- Jacobi, W. and André, K.: The vertical distribution of Radon 222, Radon 220 and their decay products in the atmosphere, *J. Geophys. Res.*, 68, 3799–3814, 1963.
- Karstens, U., Schwingshackl, C., Schmithüsen, D., and Levin, I.: A process-based  $^{222}\text{Rn}$  flux map for Europe and its comparison to long-term observations, *Atmos. Chem. Phys.*, 15, 12845–12865, doi:10.5194/acp-15-12845-2015, 2015.
- Komppula, M., Lihavainen, H., Kerminen, V.-M., Kulmala, M., and Viisanen, Y.: Measurements of cloud droplet activation of aerosol particles at a clean subarctic background site, *J. Geophys. Res.*, 110, D06204, DOI:10.1029/2004JD005200, 2005.
- Levin, I., Glatzel-Mattheier, H., Marik, T., Cuntz, M., Schmidt, M., and Worthy, D. E.: Verification of German methane emission inventories and their recent changes based on atmospheric observations, *J. Geophys. Res.*, 104, 3447–3456, 1999.
- Levin, I., Born, M., Cuntz, M., Langendörfer, U., Mantsch, S., Naegler, T., Schmidt, M., Varlagin, A., Verclas, S., and Wagenbach, D.: Observations of atmospheric variability and soil exhalation rate of Radon-222 at a Russian forest site: Technical approach and deployment for boundary layer studies, *Tellus B*, 54, 462–475, 2002.
- Levin, I., Hammer, S., Eichelmann, E., and Vogel, F.: Verification of greenhouse gas emission reductions: The prospect of atmospheric monitoring in polluted areas, *Philos. T. R. Soc. A*, 369, 1906–1924, 2011.
- Levin, I., Schmithüsen, D., and Vermeulen, A.: Assessment of  $^{222}\text{Rn}$  progeny loss in long tubing based on static filter measurements in the laboratory and in the field, *Atmos. Meas. Tech.*, 10, 1313–1321, doi:10.5194/amt-10-1313-2017, 2017.
- Mattsson, R., Helminen, V. A., and Sucksdorff, C.: Some investigations of airborne radioactivity with a view to meteorological applications, Contributions No. 58, Finnish Meteorological Office, Helsinki, 1965.
- Mattsson, R., Paatero, J., and Hatakka, J.: Automatic alpha/beta analyser for the air filter samples – absolute determination of radon progeny by pseudo-coincidence techniques, *Radiat. Prot. Dosim.*, 63, 133–139, 1996.
- Nazaroff, W. W.: Radon transport from soil to air, *Rev. Geophys.*, 30, 137–160, 1992.
- Paatero, J., Hatakka, J., Mattsson, R., and Lehtinen, I.: A comprehensive station for monitoring atmospheric radioactivity, *Radiat. Prot. Dosim.*, 54, 33–39, 1994.
- Paatero, J., Hatakka, J., and Viisanen, Y.: Concurrent measurements of airborne radon-222, lead-210 and beryllium-7 at the Pallas-Sodankylä GAW station, Northern Finland, Reports 1998:1, Finnish Meteorological Institute, Helsinki, 1998.
- Polian, G.: Les transports atmosphériques dans l'hémisphère sud et le bilan global du radon-222, PhD Thesis, University of Paris VI, France, 1986.
- Polian, G., Lambert, G., Ardouin, B., and Jegou, A.: Long-range transport of continental radon in subantarctic areas, *Tellus B*, 38, 178–189, 1996.
- Porstendörfer, J.: Properties and behaviour of radon and thoron and their decay products in the air, *J. Aerosol. Sci.*, 25, 219–263, 1994.
- Rosenfeld, M.: Modification of the Heidelberg Radon Monitor and first measurements, Diploma Thesis, Institut für Umweltphysik, Heidelberg University, 2010 (in German).
- Schery, S. D. and Huang, S.: An estimate of the global distribution of radon emissions from the ocean, *Geophys. Res. Lett.*, 31, L19104, doi:10.1029/2004GL021051, 2004.
- Schmithüsen, D., Chambers, S., Fischer, B., Gilge, S., Hatakka, J., Kazan, V., Neubert, R., Paatero, J., Ramonet, M., Schlosser, C., Schmid, S., Vermeulen, A., and Levin, I.: A European – wide  $^{222}\text{Rn}$  and  $^{222}\text{Rn}$  progeny comparison study, dataset, doi:10.1158/data/10098, 2017.
- Stockburger, H.: Continuous measurement of radon-, thorium B- and progeny activity concentration in the atmosphere, PhD Thesis, Freiburg University, 1960 (in German).
- Stockburger, H. und Sittkus, A.: Unmittelbare Messung der natürlichen und künstlichen Radioaktivität der atmosphärischen Luft, *Zeitschrift für Naturforschung*, 21, 1128–1132, 1966.
- Taguchi, S., Law, R. M., Rödenbeck, C., Patra, P. K., Maksyutov, S., Zahorowski, W., Sartorius, H., and Levin, I.: TransCom continuous experiment: comparison of  $^{222}\text{Rn}$  transport at hourly time scales at three stations in Germany, *Atmos. Chem. Phys.*, 11, 10071–10084, doi:10.5194/acp-11-10071-2011, 2011.
- Thomas, J. W. and Leclerc, P. C.: A study of the two-filter method for radon-222, *Health Phys.*, 18, 113–122, 1970.
- Van der Laan, S., Karstens, U., Neubert, R., Laan-Luijkx, I. V. D., and Meijer, H.: Observation-based estimates of fossil fuel-derived  $\text{CO}_2$  emissions in the Netherlands using  $^{14}\text{C}$ ,



- CO and  $^{222}\text{Rn}$ , *Tellus B*, 62, 389–402, doi:10.1111/j.1600-0889.2010.00493.x, 2010.
- Vardag, S. N., Hammer, S., O'Doherty, S., Spain, T. G., Wastine, B., Jordan, A., and Levin, I.: Comparisons of continuous atmospheric  $\text{CH}_4$ ,  $\text{CO}_2$  and  $\text{N}_2\text{O}$  measurements – results from a travelling instrument campaign at Mace Head, *Atmos. Chem. Phys.*, 14, 8403–8418, doi:10.5194/acp-14-8403-2014, 2014.
- Volpp, J.: Investigation of large scale atmospheric transport in Central Europe using  $^{222}\text{Rn}$ , PhD Thesis, Heidelberg University, 1984 (in German).
- Whittlestone, S. and Zahorowski, W.: Baseline radon detectors for shipboard use: development and deployment in the First Aerosol Characterization Experiment (ACE 1), *J. Geophys. Res.*, 103, 16743–16751, 1998.
- Williams, A. G., Zahorowski, W., Chambers, S., Griffiths, A., Hacker, J. M., Element, A., and Werczynski, S.: The vertical distribution of radon in clear and cloudy daytime terrestrial boundary layers, *J. Atmos. Sci.*, 68, 155–174, 2011.
- Xia, Y., Sartorius, H., Schlosser, C., Stöhlker, U., Conen, F., and Zahorowski, W.: Comparison of one- and two-filter detectors for atmospheric  $^{222}\text{Rn}$  measurements under various meteorological conditions, *Atmos. Meas. Tech.*, 3, 723–731, doi:10.5194/amt-3-723-2010, 2010.
- York, D., Evensen, N. M., Martinez, M. L., and de Basabe Delgado, J.: Unified equations for the slope, intercept, and standard error of the best straight line, *Am. J. Phys.*, 72, 367–375, 2004.